Virtual tunnels and green glass: The colors of common mirrors

Raymond L. Lee, Jr.[a)]
Mathematics and Science Division, United States Naval Academy, Annapolis, Maryland 21402

Javier Hernández-Andrés
Departamento de Óptica, Facultad de Ciencias, Universidad de Granada, Granada 18071, Spain

(Received 10 February 2003; accepted 25 July 2003)

When a pair of common second-surface plane mirrors face each other, repeated mirror-to-mirror reflections form a virtual optical tunnel with some unusual properties. One property readily analyzed in a student experiment is that the color of objects becomes darker and greener the deeper we look into the mirror tunnel. This simple observation is both visually compelling and physically instructive: measuring and modeling a tunnel's colors requires students to blend colorimetry and spectrophotometry with a knowledge of how complex refractive indices and the Fresnel equations predict reflectance spectra of composite materials. © *2004 American Association of Physics Teachers.*
[DOI: 10.1119/1.1615524]

I. INTRODUCTION

Across the centuries, mirrors have given us windows onto unusual worlds. Some of these worlds are as familiar as they are fundamentally odd: the one that lets us see our own face or the one that shows us a transposed twin of the room in which we stand. Yet the oddest mirror world may be the one found between two plane mirrors that face each other. If these mirrors are parallel (or nearly so), then looking into either of them brings us to the vertiginous edge of a visual tunnel that seems to recede endlessly into the virtual distance.

We call this phenomenon of repeated mirror reflections a *mirror tunnel*, and here we are interested in how one formed by two common mirrors transforms the colors of reflected objects. (We define *common mirrors* as inexpensive second-surface plane mirrors such as those found in homes.) Understanding these transformations can teach students not only about geometrical optics and spectral transfer functions, but also how knowing the complex refractive indices of the metal backing and glass in such mirrors lets us predict their reflectance spectra via the Fresnel equations.[1] In a student experiment, two especially instructive (and surprising) results are that common mirrors are not spectrally neutral reflectors, and their reflectance spectra depend on the absorbing and reflecting properties of both the glass substrate and its metal backing.

Because mirror tunnels are so visually compelling, we use them as a pedagogical tool in this paper. In Sec. II we describe how to set up a mirror tunnel and observe its color shifts, and in Sec. III we discuss the measured reflectance spectra of some common mirrors and show how we use such spectra to calculate the chromaticity trends seen in mirror tunnels. In Sec. IV we use existing data on the complex refractive indices of silver and soda–lime silica glasses in a simple model that calculates the reflectance spectra and chromaticities for these mirrors. At a minimum, students should already be familiar with the optical significance of the materials' absorption, reflection, and transmission spectra. For deeper insights, they also should understand how such purely physical properties are translated into the psychophysical metric of colorimetry. A very readable introduction to the colorimetric system of the Commission Internationale de l'Eclairage (CIE) is given in Ref. 2.

II. THE MIRROR TUNNEL DEMONSTRATION

One well-designed mirror tunnel is seen in Granada, Spain's Science Museum.[3] This virtual tunnel is produced simply by placing two tall mirrors parallel to and facing each other (see Fig. 1). Viewers look at one mirror through two small holes in the back of the other mirror; the holes are spaced to match the average distance between human eyes. This viewing geometry avoids the problem that can occur if the viewer's head is between the two mirrors, where it can block the angularly smallest, most interesting regions of the mirror tunnel.

On looking through the eyeholes, one sees a long progression of ever-smaller reflected images of the two mirrors that plunges into the virtual distance, thus giving the illusion of an infinite tunnel (Fig. 2). If the mirrors are not exactly parallel (as is true in Fig. 2), then the tunnel curves in the same direction that the mirrors tilt toward each other.[4] After relishing the vertiginous thrill of this virtual tunnel, we find another, subtler feature: the farther we look into the tunnel, the greener and darker its reflected objects appear. To track this color and brightness shift in Fig. 2, we put a photographer's gray card at the base of one mirror. Although the card's image becomes progressively darker and more yellow–green with successive reflections, no such shifts occur for distant real objects seen by a single reflection in either mirror.

This simple observation lies at the heart of our paper, and it begs the question that students must answer: why do repeated reflections change the mirror images' color and brightness? Geometrical optics is silent on this point, because it predicts only the images' location and size. Thus, to explain the brightness and color changes, we must consider the physical optics of common mirrors. Because color depends on spectral variability, we start by examining the spectral reflectances and transmissivities of the metal and glass used to make these mirrors.

III. MEASURED REFLECTANCE SPECTRA AND COLORS OF COMMON MIRRORS

Common household mirrors have long been made by depositing a thin film of crystalline silver on the rear surface of float-process flat glass.[5] This silver film is optically thick (minimum thickness $\sim 10\ \mu$m), and its rear surface is protected from oxidation and abrasion by successive films of

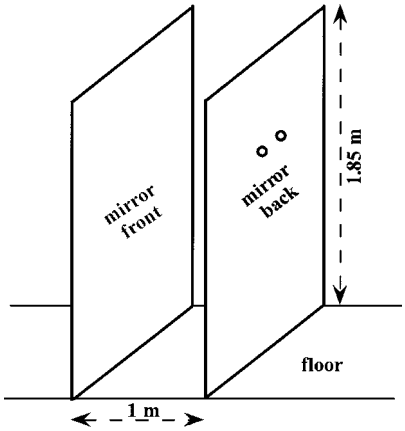

Fig. 1. Schematic diagram of the mirrors used to produce the virtual mirror tunnel photographed in Fig. 2. The circles on the right mirror are eyeholes through which observers view the mirror tunnel.

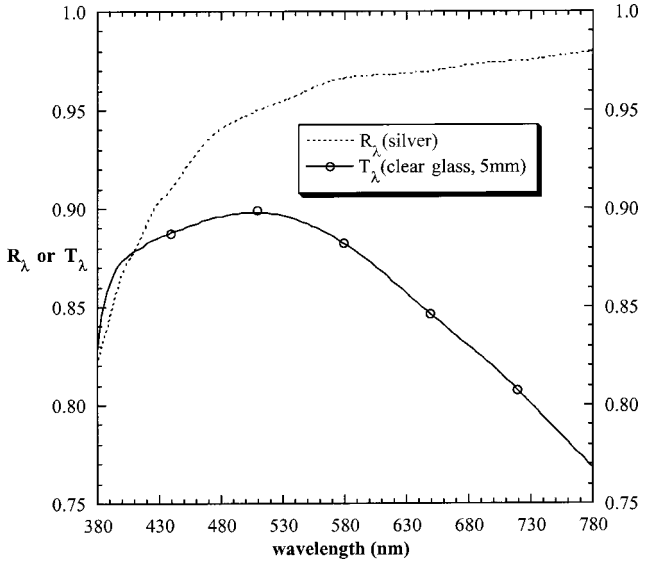

Fig. 3. Normal-incidence spectral reflectances R_λ for optically thick silver and spectral transmissivities T_λ for a 5 mm thick layer of nominally clear soda–lime silica (SiO_2) glass. The optical properties of each material are considered separately here (that is, they are not combined as a mirror), and the incident medium is air.

copper and lacquer. The polished glass itself is usually clear soda–lime silica whose constituents (by weight) are about 72% SiO_2, 14% Na_2O ($+K_2O$), 9% CaO, 3% MgO, 1% Al_2O_3, and variable, smaller amounts of Fe_2O_3 ($<1\%$).[6,7] Other backing metals (for example, aluminum) and special ''colorless'' (that is, lower iron oxide content) or tinted glass can be used to change a mirror's reflectance spectrum appreciably.

Nonetheless, a soda–lime silica glass substrate with silver backing forms the optical core of most common mirrors. Figure 3 shows the reflectance and transmission spectra of these two materials in air at visible wavelengths λ ($380 \leqslant \lambda \leqslant 780$ nm).[8,9] Although the glass transmits most at 510 nm (a green), its broad transmission maximum only imparts a pastel greenish cast to white light, even after it has been transmitted through several centimeters of the glass. This greenish cast is best seen by looking obliquely through a plate of common glass, bearing in mind that refractive dispersion can complicate the colors that students see. In other words, students should learn to distinguish between the uniform green or blue–green that results from glass absorption and the many prismatic colors that result from glass refraction. In contrast, although Fig. 3's silver spectrum shows a fairly steep decrease in spectral reflectance R_λ below 460 nm, at longer wavelengths the metal reflects much more spectrally uniformly.

Fig. 2. Mirror tunnel photographed at the Science Museum in Granada, Spain. The large white circle framing the mirror tunnel is one of Fig. 1's eyeholes, which also appear as small dark circles within the tunnel itself.

When we form a composite common mirror from these two materials, what reflectance spectra result? Figure 4 shows some representative spectra both from Granada's Science Museum mirrors and from common mirrors in our own laboratories and homes ($400 \leqslant \lambda \leqslant 700$ nm, measured in 10 or 5 nm steps). We measured these spectra at normal incidence using either of two portable spectrophotometers: a Minolta CM-2022 or a HunterLab UltraScan.[10] In Fig. 4, all spectral reflectances except those labeled ''R_λ (lab 1)'' were measured with the Minolta CM-2022. Given the instruments' designs, these spectra necessarily include both external specular reflections from the mirror glass and multiple reflections from within the mirror.

One of Fig. 4's most striking features is how much the overall reflectance R varies from mirror to mirror (and, as our measurements show, even within a given mirror); mean R values range from 80.5% for the ''museum 1'' mirror to 95.6% for the ''home 2'' mirror. Although some of this variability may be attributed to spectrophotometer errors, more variability likely comes from differences in the mirrors' original fabrication.

Nevertheless, Fig. 4's spectra all have similar shapes: they peak on average at 545 nm, a yellowish green. To restate these spectral differences in colorimetric terms, after a single reflection of a spectrally flat illuminant (the equal-energy spectrum),[11] the *most* dissimilar mirrors in Fig. 4 (the museum 1 and home 2 mirrors) slightly change that illuminant's color into two new colors. However, these two colors differ by only 14% more than the local MacAdam just-noticeable

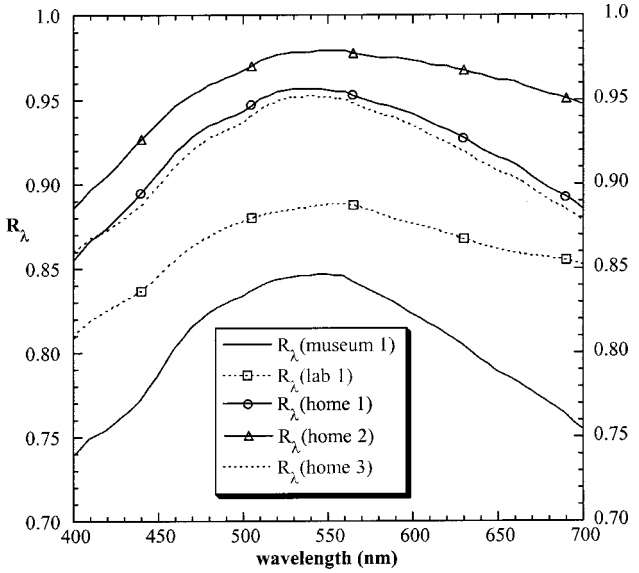

Fig. 4. Measured spectral reflectances R_λ for several common mirrors. All measurements were made at normal incidence and include external specular reflections from the mirror glass and multiple reflections from within the mirror.

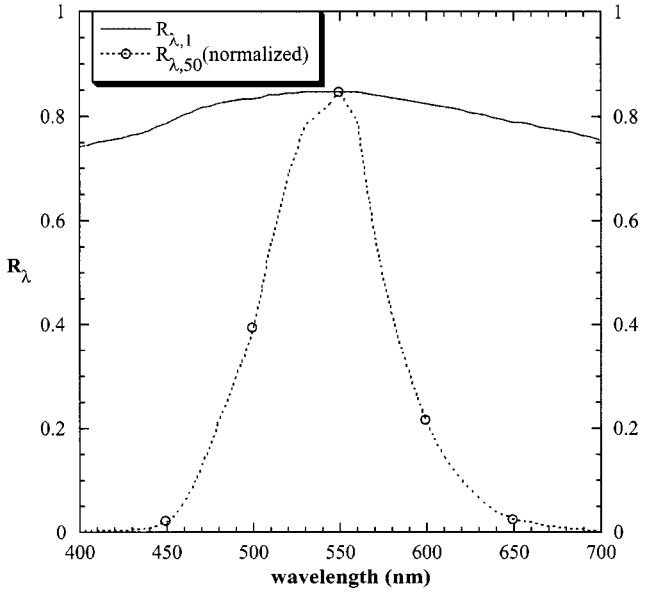

Fig. 5. Effective spectral reflectances for the museum 1 mirror in Fig. 4 after one ($R_{\lambda,1}$) and 50 ($R_{\lambda,50}$) mirror-to-mirror reflections. To emphasize the $R_{\lambda,50}$ spectrum's greatly increased spectral selectivity, we normalize it to have the same maximum as the $R_{\lambda,1}$ spectrum. In reality, after 50 mirror-to-mirror reflections, the mean reflectance and reflected luminance decrease by factors of 11 620 and 5780, respectively.

difference.[12] In other words, after a single reflection, although many observers might be able to distinguish between colors reflected by Fig. 4's most dissimilar mirrors when viewed side by side, this is by no means certain. Thus, the color shifts caused by Fig. 4's very different-looking reflectance spectra will appear nearly identical.

Yet each mirror's color shift is by itself only marginally perceptible. Using the same equal-energy illuminant as before, we find that after one reflection, even the most spectrally selective mirror in Fig. 4 (the museum 1 mirror) increases that light's colorimetric purity by $<3\%$ or ~ 2.7 just-noticeable differences. More significantly for the mirror tunnel, the dominant wavelength of this low-purity reflected light is 560 nm, a yellow–green. In the mirror tunnel, of course, light undergoes not one but many reflections between the two mirrors before reaching our eyes. Energy conservation requires the mirror tunnel's effective spectral reflectance $R_{\lambda,N}$ after N reflections to be

$$R_{\lambda,N}=(R_{\lambda,1})^N, \tag{1}$$

where $R_{\lambda,1}$ is as given above, the spectral reflectance after one reflection by a mirror.

Figure 5 shows the pronounced spectral effects of 50 reflections by the Science Museum mirrors. The 50th reflection has a much weaker and spectrally narrower reflectance spectrum than the first reflection. Obviously, this makes colors in the mirror tunnel's most ''distant'' images darker and more saturated. In particular, 50 reflections by the museum 1 mirror give a white object a dominant wavelength ~ 552 nm and colorimetric purity $\sim 71\%$,[13] compared with the 3% purity resulting from one reflection. Equally dramatic is the fact that the white object's reflected luminance is reduced by a factor of 5780 after 50 reflections.[14]

Between these extremes, the mirror tunnel's luminances and chromaticities follow easily predicted, although distinctly nonlinear, paths. To provide a context for these chromaticities, Fig. 6 shows the entire CIE 1931 x, y chromaticity diagram,[2] to which we have added a dashed chromaticity locus for blackbody (or Planckian) radiators. The dimensionless CIE 1931 chromaticity coordinates x, y are derived from psychophysical experiments in which subjects matched the colors of test lights by mixing red, green, and blue reference lights in varying intensities. To a first approximation, the x coordinate represents the relative amounts of green and red in a color, and the y coordinate indicates the relative amounts of green and blue.

The chromaticity diagram's curved border in Fig. 6 consists of monochromatic spectrum colors that increase clock-

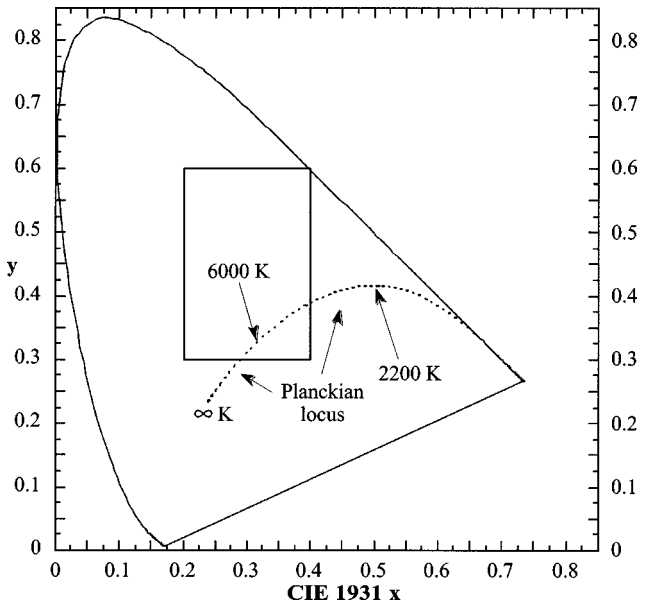

Fig. 6. CIE 1931 x, y chromaticity diagram, to which is added the curved chromaticity locus of blackbody (or Planckian) radiators. The rectangular box that straddles the Planckian locus is the region shown in Fig. 7; its upper right corner just touches the horseshoe-shaped spectrum locus.

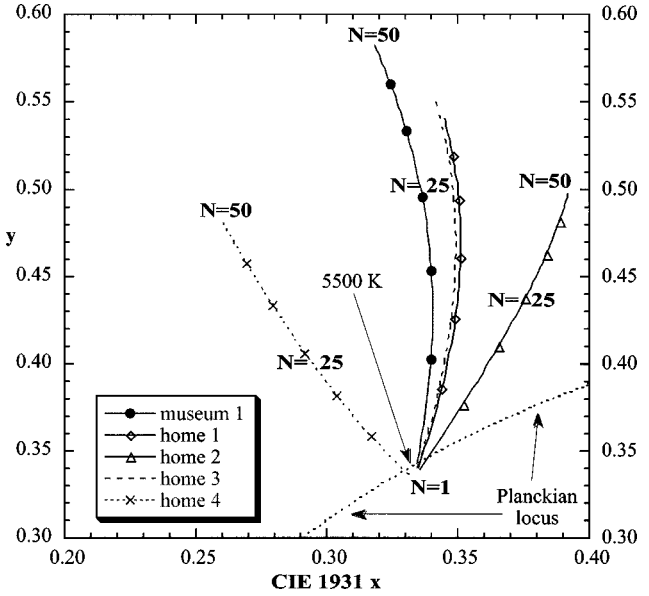

Fig. 7. CIE 1931 x, y chromaticity curves for a white object seen after N mirror-to-mirror reflections in a mirror tunnel. The mirrors are those whose measured R_λ are plotted in Fig. 4, plus one additional mirror (the home 4 curve). In order to show as much detail as possible, the x, y scaling is not isotropic (unlike Fig. 6).

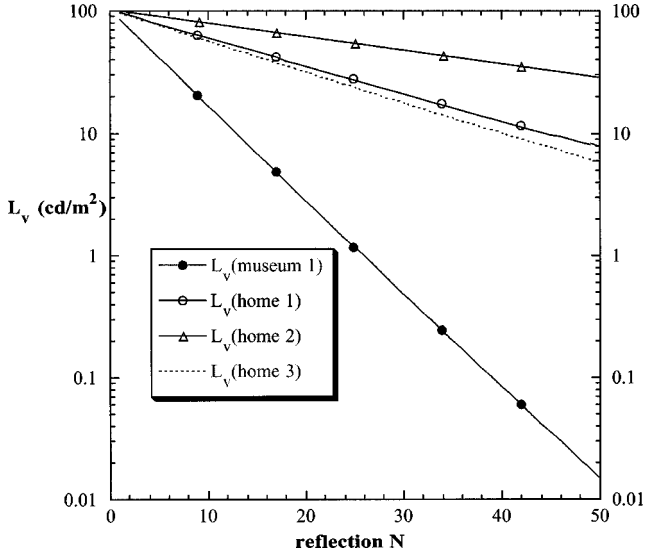

Fig. 8. The reflected mirror-tunnel luminance L_ν (arbitrary maximum value) decreases nearly logarithmically with an increasing number of mirror-to-mirror reflections N. The mirrors are those whose R_λ are plotted in Fig. 4.

wise from short wavelengths at the diagram's left vertex (near $x=0.175$, $y=0.0$) to long wavelengths at its right vertex (near $x=0.735$, $y=0.265$). This curved part of the border is called the *spectrum locus*. A straight line connects these two spectral extremes, and mixtures of monochromatic red and blue along it generate purples. Thus, purples are not spectrum colors proper (they are not monochromatic), but they are the purest possible colors that link the ends of the visible spectrum. One point in Fig. 6's interior is a white or *achromatic stimulus*, and for the equal-energy illuminant its chromaticity coordinates are $x=0.333\,33$, $y=0.333\,33$. We can form any other color by additively mixing a specific amount of this achromatic stimulus with a spectrum color (or a purple). An arbitrary color's *dominant wavelength* is found by extending a straight line from the achromatic stimulus through the arbitrary color and then on to intersect the spectrum locus. The monochromatic spectrum color at this intersection defines the arbitrary color's dominant wavelength. Furthermore, the arbitrary color's fractional distance between white and its spectrum color defines its *colorimetric purity*.

Figure 7 expands the boxed area in Fig. 6, and in it we plot chromaticity curves for a white object seen after N mirror-to-mirror reflections by the mirrors in Fig. 4. Each curve in Fig. 7 is constructed by repeatedly drawing from the chromaticity coordinates x_N, y_N for the R_N reflection to x_{N+1}, y_{N+1} for the R_{N+1} reflection ($1\leqslant N\leqslant 50$). We calculate each x_N, y_N by multiplying the equal-energy illuminant's power spectrum by a white object's constant R_λ and the mirrors' changing $R_{\lambda,N}$. To show the maximum color range for mirror tunnels resulting from our measured spectra, we substitute in Fig. 7 a slightly more greenish common mirror ("home 4") for the "lab 1" mirror in Fig. 4. Note that all colorimetric calculations given here can be done easily in an electronic spreadsheet that contains mirror spectra and the human color-matching functions.[15]

As expected, Fig. 7's chromaticities grow steadily purer with increasing N. However, for the largest N, the most distant colors in the tunnel are difficult (or impossible) to see because they are so dark. In fact, Fig. 8 shows that the reflected luminance L_ν decreases nearly logarithmically with N, as one would expect from Eq. (1).[16] Figure 8 does not include the "home 4" L_ν shown in Fig. 7 because they would overlie the L_ν of museum 1. Note that after 50 reflections the latter mirror not only yields the darkest colors (Fig. 8), but also the purest ones (Fig. 7). This decreased brightness is no coincidence, because increased spectral purity necessarily comes at the price of reduced luminance for nonfluorescing reflectors (see Fig. 4).

IV. MODELING MIRROR-TUNNEL COLORS

One of the most instructive and satisfying aspects of the mirror–tunnel exercise for students is that they can simulate a fairly complex optical system with only modest mathematical effort. We start with the facts that a second-surface mirror's spectral reflectance R_λ depends on the mirror surface's preparation, the illuminant's incidence angle and polarization state, the glass thickness and composition, and the optical properties of the metal itself. We then base our model on the following assumptions.

(1) The mirror is a polished flat substrate of soda–lime silica (SiO_2) glass that is 5 mm thick and is backed by an optically thick silver (Ag) film. This glass matches the thickness of the mirror glass shown in Fig. 2.

(2) We assume normal incidence for all reflections. Strictly speaking, the eyeholes in an actual mirror tunnel (see Figs. 1 and 2) keep us from seeing normal-incidence reflections between the two mirrors, but this fact only negligibly affects the relevance of the color and luminance trends simulated here.

(3) We include the effects on R_λ of 5 reflections within each mirror (see Fig. 9); higher-order internal reflections contribute almost nothing to R_λ. However, we exclude interference among the internally reflected rays because the mirror glass is sufficiently thick (~8620 times the mean vis-

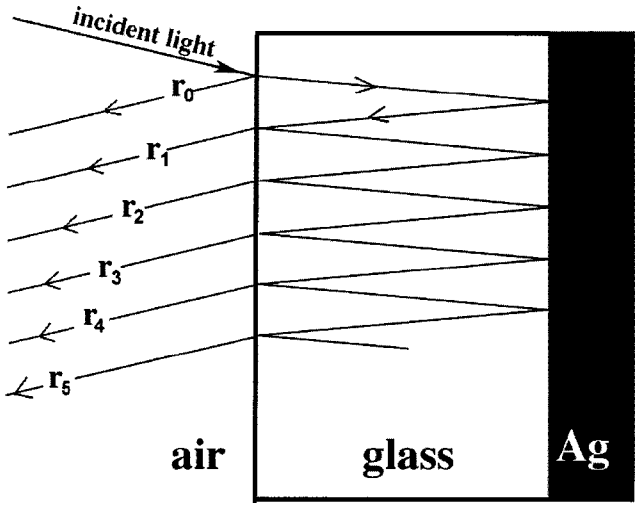

Fig. 9. The specular external reflection, r_0, and multiple internal reflections $r_1 \cdots r_5$ that contribute to the measurable reflectance R of a composite glass/silver second-surface mirror. For clarity, these reflections are shown at non-normal incidence.

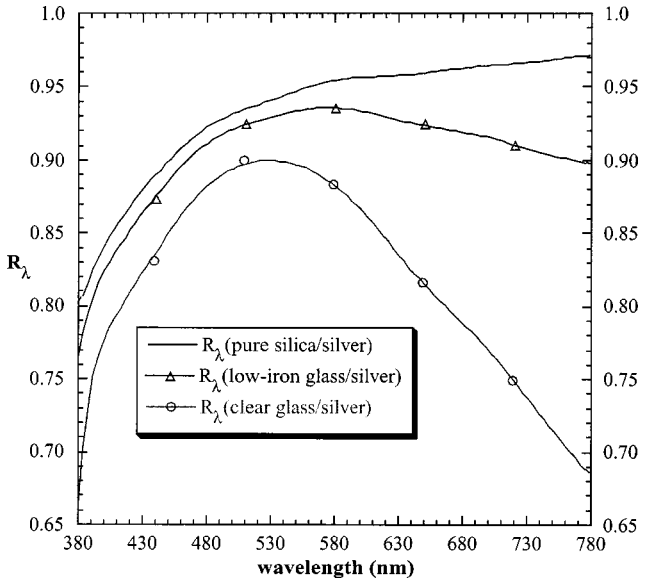

Fig. 10. Simulated spectral reflectances R_λ for several types of second-surface glass mirrors, modeled using Eqs. (2)–(5). Each simulation assumes normal incidence and includes external specular reflections from the mirror glass, multiple reflections from within the mirror, and a 5 mm thick glass substrate.

ible λ) so that its optical pathlengths are far greater than the illuminant's coherence length.[17] Thus we add the intensities, rather than the amplitudes, of successive internal reflections.

(4) As was true in Sec. III, we assume an unpolarized, equal-energy illuminant.

During the light's traversal of the mirror, it variously undergoes absorption within a medium or reflection and transmission at an interface between two media. Note that all the following equations are implicit functions of wavelength. At the air–glass interface, external specular reflection r_0 is given by the normal-incidence Fresnel equation:[1]

$$r_0 = r_{\text{air/glass}} = \frac{(n_{\text{glass}} - n_{\text{air}})^2 + k_{\text{glass}}^2}{(n_{\text{glass}} + n_{\text{air}})^2 + k_{\text{glass}}^2}, \tag{2}$$

where n_{glass} and k_{glass} are the real and imaginary components of the refractive index of soda–lime silica glass,[7,8] and $n_{\text{air}} = 1$ at visible wavelengths.

Transmittance through the glass T_{glass} is modeled by the Lambert–Bouguer–Beer exponential absorption law:

$$T_{\text{glass}} = \exp(-4\pi d k_{\text{glass}}/\lambda), \tag{3}$$

where d is the mirror glass' thickness. Normal-incidence reflection at the glass/Ag interface is given by

$$r_{\text{glass/Ag}} = \frac{(n_{\text{glass}} - n_{\text{Ag}})^2 + (k_{\text{glass}} - k_{\text{Ag}})^2}{(n_{\text{glass}} + n_{\text{Ag}})^2 + (k_{\text{glass}} + k_{\text{Ag}})^2}, \tag{4}$$

where n_{Ag} and k_{Ag} are the real and imaginary components of the refractive index of silver.[9] Here r denotes component reflectances from within the mirror, in contrast to their sum R, the reflectance that we can measure with a spectrophotometer.

Using Eqs. (2)–(4), we add the external specular and multiple within-mirror reflections as follows (see Fig. 9):

$$R = r_0 + \sum_{j=1}^{5} r_j, \tag{5}$$

where $r_j = (1 - r_{\text{air/glass}})^2 r_{\text{air/glass}}^{j-1} T_{\text{glass}}^{2j} r_{\text{glass/Ag}}^{j}$ is the jth internally reflected contribution to R by light that is (a) initially transmitted from air to glass and, ultimately, from glass to air (the factor of $(1 - r_{\text{air/glass}})^2$), (b) reflected internally at the air/glass interface if $j > 1$ (the factor of $r_{\text{air/glass}}^{j-1}$), (c) transmitted twice through the glass en route to and from the silver backing (the factor of T_{glass}^{2j}), and (d) reflected at the silver backing (the $r_{\text{glass/Ag}}^{j}$ factor). Note that for all j, $r_j \gg r_{j+1}$, which means that each successive internal reflection makes a much smaller contribution to the observed R.

At non-normal incidence and reflection angles, the external reflection r_0 and internal reflections r_j from slightly different directions actually contribute to the observed R, but the small relative size of r_0 (~0.04 at visible wavelengths) and the rapid decrease in r_j means that r_1 dominates R. Thus, common mirrors function much as desired—most of their reflected luminance comes from a single reflection by the mirror's metal backing. We include the higher-order reflections here for completeness and because they do contribute to a second-surface mirror's images, even if only by slightly degrading their quality.

Figure 10 shows R_λ predicted by our model for three composite mirrors, each using the same silver backing but a different glass. In addition to the clear and low-iron soda–lime silica glasses,[8] Fig. 10 also plots the simulated R_λ for a mirror whose glass is pure silica.[18,19] Not surprisingly, the impurity-free silica mirror is the least absorbing of the three, and so its reflectance spectrum most closely resembles that of the silver backing (Fig. 3). With increasing amounts of iron oxide in the glass substrate, the mirrors not only have lower mean R, but also become more spectrally selective. Thus, the two mirror tunnels with the most dissimilar colors should be those produced by the least and most absorbing mirror glass (pure silica and clear glass, respectively).

We see this trend in the chromaticity diagram of mirror tunnels predicted for our simulated mirrors (see Fig. 11). To aid the comparison with mirror tunnels produced by actual common mirrors, we repeat the chromaticity curves from Fig. 7 in Fig. 11. In addition, we include the mirror tunnel for

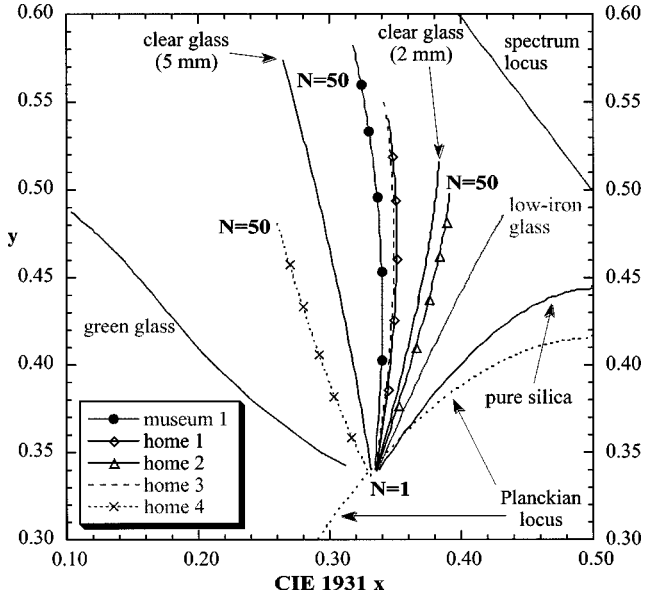

Fig. 11. Chromaticity curves for a white object seen after N mirror-to-mirror reflections in a mirror tunnel produced by our measured (Fig. 4) and simulated (Fig. 10) common mirrors, plus curves for simulated mirrors made either with slightly greenish glass (green glass curve) or clear glass that is 2 mm thick [clear glass (2 mm) curve]. See Fig. 7 for a closer view of the measured mirror tunnels' chromaticities.

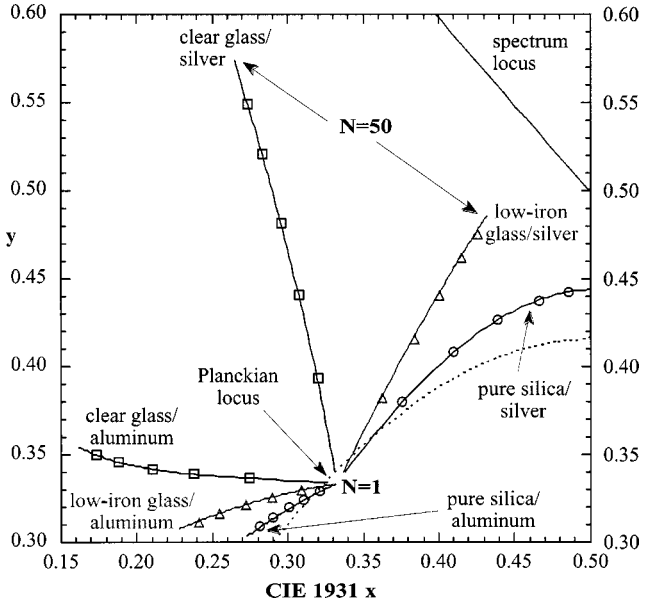

Fig. 12. The colorimetric consequences of changing the backing metal in several of the simulated mirrors shown in Fig. 11. Replacing silver with aluminum rotates each mirror–tunnel chromaticity curve counterclockwise (that is, toward shorter wavelengths), and the amount of rotation increases with decreasing absorption by the mirror glass.

a fourth simulated mirror, this one made using the greenish soda–lime silica glass from Ref. 8. Note that pure silica produces a mirror tunnel whose chromaticities quickly curve toward the yellow as N increases. This curvature occurs because pure silica absorbs very little, and thus the repeated reflections merely serve to increase the purity of silver's slightly yellowish reflectance spectrum. However, the mirror tunnels predicted for our other simulated glasses in Fig. 11 have chromaticity curves that point toward shorter dominant wavelengths (that is, toward the greens) as the mirror glass' iron oxide content increases (shifting from pure silica to the greenish glass). Table I quantifies these colorimetric trends for $N=25$ reflections.

Students can glean several insights from Fig. 11. First, mirror–tunnel colors depend on the properties of *both* the backing metal and the glass substrate, as seen in the tunnels' chromaticity curves when we change either mirror component. To make this subtle point, we suggest that students first examine samples of polished silver, aluminum, and low-iron and ordinary clear window glass. They will see that the metals look similar, as do the two glasses. Next, have them calculate how much changing the mirror's backing metal changes the mirror–tunnel colors. The result is startling: Fig. 12 shows that if aluminum[20] is used rather than silver, the simulated mirror tunnels in Fig. 11 shift markedly toward shorter wavelengths. Thus, compared to their silver counterparts, aluminum-backed mirrors yield chromaticity curves that are rotated counterclockwise around the point marked $N=1$. Furthermore, the amount of rotation varies inversely with mirror-glass absorption (that is, weakly absorbing pure silica yields a larger shift than does clear glass). This shift toward shorter dominant wavelengths occurs because aluminum has a slightly bluish reflectance spectrum.

Table I. Dominant wavelengths, colorimetric purities, and approximate CIE color names for a white object seen in the simulated mirror tunnels in Fig. 11 after $N=25$ mirror-to-mirror reflections. Each mirror is backed with silver, and the light source is the equal-energy illuminant. Unless noted otherwise, the mirror glass thickness is 5 mm.

	Dominant wavelength (nm)	Purity (%)	CIE color name
Pure silica	580	59.7	Yellow
Low-iron glass	572	52.7	Greenish yellow
Clear glass (2 mm)	566	48.0	Yellow green
Clear glass	540	35.1	Yellowish green
Greenish glass	501	57.9	Green

Second, if we reduce the mirror glass thickness from 5 to 2 mm (the smaller value is found in some home mirrors), this reduction rotates a mirror's chromaticity curve clockwise in Fig. 11, and the amount of rotation increases with k_{glass}. Thus, a chromaticity curve's degree of rotation increases as intrinsic absorption by the mirror glass increases, and the rotation caused by reduced glass thickness is toward longer wavelengths (that is, toward the chromaticity curve that would result from the silver backing alone). Figure 11 shows the rotation that results from replacing the 5 mm substrate of clear glass with one that is 2 mm thick. However, no perceptible shift occurs if we reduce the thickness of the pure silica mirror glass to 2 mm, because a 5 mm layer absorbs (and colors) so little of the incident light. When students calculate and ponder such dramatic colorimetric shifts, it will reinforce for them just how much the appearance of composite materials depends on each material's optical properties.

Third, Fig. 11 indicates the power of even a simple model to explain the complicated world of everyday appearances—the measured colors of a range of common mirrors closely match those simulated for similar mirrors made of silver and clear soda–lime silica glass. Finally, students can learn that spectrally selective absorption from multiple reflections in glass and mirrors has many practical implications in research

areas ranging from signal loss in fiber optic cables[19] to spectroscopic analysis of gases within optically resonant cavities.[21]

V. SUMMARY

Mirror tunnels have the twin advantages of being visually and intellectually intriguing. Thus, an experiment that lets students explore the relationship between the exotic visual world of the mirror tunnel and the measured and modeled optical properties of common mirrors makes for an instructive, appealing bridge between geometrical and physical optics. The path that we have taken here has the virtue of using readily observed phenomena (the mirror tunnel's color and brightness trends) to develop and test a simple, but fairly rigorous, optical model that explains them. Along the way, students will find that seemingly abstruse ideas such as colorimetry, the Fresnel equations, and complex refractive indices can be combined to explain everyday visual experience.

ACKNOWLEDGMENTS

We are grateful to the Science Museum of Granada, Spain for permitting us to photograph its mirror tunnel demonstration. Several agencies generously funded this research. Lee was supported by United States National Science Foundation Grant No. ATM-0207516 and by the United States Naval Academy's Departments of Physics and Mathematics. Hernández-Andrés was supported by Spain's Comisión Interministerial de Ciencia y Tecnología (CICYT) under research grant No. BFM 2000-1473.

[a]Electronic mail: raylee@usna.edu

[1]M. V. Klein and T. E. Furtak, *Optics*, 2nd ed. (Wiley, New York, 1986), pp. 263–307.

[2]R. S. Berns, *Billmeyer and Saltzman's Principles of Color Technology*, 3rd ed. (Wiley, New York, 2000), pp. 44–66.

[3]Parque de las Ciencias, Avda. del Mediterráneo s/n, 18006 Granada, Spain, ⟨http://www.parqueciencias.com⟩.

[4]Thus in Fig. 2, the ascending ''staircase'' of floor images arises because the mirrors' tops are closer than their bases. The mirror tunnel's curvature is useful in itself for discussing the geometrical optics of plane mirrors and the behavior of their virtual images.

[5]B. Schweig, *Mirrors: A Guide to the Manufacture of Mirrors and Reflecting Surfaces* (Pelham Books, London, 1973), pp. 3–4, 23–77.

[6]H. G. Pfaender and H. Schroeder, *Schott Guide to Glass* (Van Nostrand Reinhold, New York, 1983), pp. 45, 66.

[7]T. Uchino, K. Nakaguchi, Y. Nagashima, and T. Kondo, ''Prediction of optical properties of commercial soda–lime–silicate glasses containing iron,'' J. Non-Cryst. Solids **261**, 72–78 (2000).

[8]M. Rubin, ''Optical properties of soda lime silica glasses,'' Sol. Energy Mater. **12**, 275–288 (1985).

[9]*Handbook of Optical Constants of Solids*, edited by E. D. Palik (Academic, Orlando, FL, 1985), Table IX, p. 356.

[10]CM-2022 spectrophotometer from Minolta Corporation, 101 Williams Drive, Ramsey, NJ 07446; HunterLab UltraScan spectrophotometer from HunterLab Associates, Inc., 11491 Sunset Hills Road, Reston, VA 20190-5280. Both instruments were calibrated shortly before we measured the spectra in Fig. 4.

[11]Although the equal-energy illuminant is rarely encountered, we use its spectral simplicity to help us isolate the colorimetric effects of R_λ in creating the mirror tunnel's colors. For more realistic illuminants (for example, incandescent lighting), the mirror tunnel's chromaticities depend on the wavelength-by-wavelength multiplication of R_λ and a more complicated power spectrum.

[12]G. Wyszecki and W. S. Stiles, *Color Science: Concepts and Methods, Quantitative Data and Formulae*, 2nd ed. (Wiley, New York, 1982), pp. 306–310. Here we follow convention and set the just-noticeable difference equal to the semimajor axis length of the MacAdam color-matching ellipse at the relevant chromaticity. For the equal-energy illuminant, this chromaticity is CIE 1931 $x=0.333\,33$, $y=0.333\,33$. We define chromaticity coordinates and other basic CIE metrics elsewhere in the main text.

[13]Dominant wavelengths and purities are measured with respect to the equal-energy illuminant's chromaticity. Here we define a white object as a diffuse reflector with constant R_λ at visible wavelengths, say $R_\lambda=0.9$; a photographer's white card approximates this behavior.

[14]Because each of the ~12 reflected gray-card images visible in Fig. 2 occurs after one pair of reflections between the two mirrors, $N=24$ total reflections contribute to the color and brightness of its smallest gray card image. To measure the relative luminance (or radiance) of the $N=24$ mirror reflection, we restrict the spectroradiometer's field of view to the 12th smallest image of some easily recognized object in the mirror tunnel (for example, the gray card in Fig. 2). Then we divide this reading by the luminance or radiance of the object seen directly (the $N=0$ image). Given the large luminance reductions involved, $N=50$ reflections is a generously large upper limit on the visibility of mirror tunnels formed by common mirrors.

[15]On request, we will gladly provide readers with as many of our measured mirror spectra as desired, plus instructions on how to use this data in colorimetric calculations. We also can give readers smoothly interpolated complex refractive indices of glasses and metals in a form that is suitable for simulating mirrors' chromaticities (see the model of Sec. IV).

[16]The relationship between L_ν and N is not quite log-linear because luminance is calculated by a spectral integral that includes the changing shape of the mirrors' $R_{\lambda,N}$. If a mirror's original spectral reflectances $R_{\lambda,1}$ were *completely* uniform, then both the reflected luminance and radiance would decrease exactly logarithmically with increasing N.

[17]J. Hernández-Andrés, E. M. Valero, J. L. Nieves, and J. Romero, ''Fizeau fringes at home,'' Am. J. Phys. **70**, 684–688 (2002).

[18]For the complex refractive indices of pure silica, see Ref. 9, Table X, pp. 759–760.

[19]We use data on pure silica's very weak visible-wavelength absorption found in B. Keck, R. D. Maurer, and P. C. Schultz, ''On the ultimate lower limit of attenuation in glass optical waveguides,'' Appl. Phys. Lett. **22**, 307–309 (1973).

[20]For the complex refractive indices of metallic aluminum, see Ref. 9, Table XII, pp. 398–399.

[21]*Cavity-Ringdown Spectroscopy: An Ultratrace-Absorption Measurement Technique*, edited by K. W. Busch and M. A. Busch (American Chemical Society, Washington, DC, 1999).